

Growth and Properties of LiNbO₃:Mg,B Crystals

I. V. Biryukova^a, I. N. Efremov^a, O. E. Kravchenko^a, V. A. Sandler^a,
N. A. Teplyakova^{a, *}, and M. N. Palatnikov^a

^a Tananaev Institute of Chemistry and Technology of Rare Elements and Minerals (separate subdivision), Kola Scientific Center (Federal Research Center), Russian Academy of Sciences, Apatity, Murmansk oblast, 184209 Russia

*e-mail: n.tepliakova@ksc.ru

Received January 14, 2022; revised March 10, 2022; accepted March 11, 2022

Abstract—A technologically feasible process has been proposed for the preparation of a LiNbO₃:Mg,B growth charge from a Li₂CO₃ + Nb₂O₅ + MgO + H₃BO₃ mixture. Using such a growth charge, we have grown LiNbO₃:Mg,B crystals with a highly uniform dopant distribution. High-speed evaluation of optical homogeneity has shown that the LiNbO₃:Mg,B crystals have high optical quality. Using amplitude–frequency response and d_{333} piezoelectric modulus measurements, we have demonstrated a high degree of unipolarity of the LiNbO₃:Mg,B crystals. The optical damage resistance and homogeneity of the LiNbO₃:Mg,B crystals have been assessed using photoinduced light scattering and laser conoscopy. The results suggest that LiNbO₃:Mg,B crystals with a weak photorefractive effect can be regarded as a new optical material for laser light conversion.

Keywords: lithium niobate crystals, doping, scattering centers, piezoelectric modulus, degree of unipolarity

DOI: 10.1134/S0020168522070068

INTRODUCTION

Physical characteristics of lithium niobate (LiNbO₃) crystals, which are among nonlinear optical materials of greatest practical importance, are commonly varied via changes in their stoichiometry ($R = [\text{Li}]/[\text{Nb}]$) or by doping [1]. Doping with impurities (Mg, Zn, Gd, In, Sc, and others) is an effective approach for reducing the photorefractive effect in LiNbO₃ crystals [1, 2]. Their optical damage resistance rises stepwise at rather high (threshold) dopant concentrations [1, 2]. For example, the threshold for LiNbO₃:Mg crystals is ~4.0–5.3 mol % Mg (~0.7–0.93 wt % Mg) [3–6]. However, such doping typically leads to chemical inhomogeneity of crystals.

Nonmetallic ions (such as B³⁺) are incapable of occupying the oxygen octahedra in LiNbO₃ crystals. At the same time, our previous results demonstrate that, when used as a flux in crystal growth, boron oxide influences the structure and physicochemical characteristics of the melt, which makes it possible to obtain nearly stoichiometric LiNbO₃ crystals from a congruent melt [7–9]. According to mass spectrometry data, boron concentration in LiNbO₃:B crystals is extremely low: ~10⁻⁵ to 10⁻⁴ wt % [7].

Optical characteristics of LiNbO₃ crystals can be significantly improved by codoping with Mg, an impurity capable of suppressing the photorefractive effect, and B³⁺, a nonmetallic element that markedly

improves the optical homogeneity of LiNbO₃ crystals. Masloboeva et al. [10] demonstrated the feasibility of growing optically and chemically homogeneous LiNbO₃:Mg,B crystals from a homogeneously doped growth charge prepared from a mixture of Li₂CO₃ and Nb₂O₅:Mg,B as a precursor.

The objectives of this work were to grow optically and chemically homogeneous LiNbO₃:Mg,B crystals from a growth charge prepared from a Li₂CO₃ + Nb₂O₅ + MgO + H₃BO₃ mixture and assess the chemical homogeneity, optical quality, optical damage resistance, and degree of unipolarity of the crystals.

EXPERIMENTAL

A granulated Mg–B codoped growth charge of congruent composition ($[\text{Li}_2\text{O}]/[\text{Nb}_2\text{O}_5] = 0.946$) was prepared by a synthesis/granulation method from a Li₂CO₃ + Nb₂O₅ + MgO + H₃BO₃ mixture. Li₂CO₃ and Nb₂O₅ were prepared for synthesis in accordance with recommendations by Palatnikov et al. [11]. MgO was preannealed at ~850°C for 6 h. After mechanical activation of the starting materials for 24 h in a tumbling drum, the Li₂CO₃ + Nb₂O₅ + MgO + H₃BO₃ mixture was placed in a platinum crucible and slightly compacted. The granulation temperature and holding time were ~1235°C and 5 h. The mixture was heated at a rate of ~200°C/h. The percentage of boron in the growth charge and crystals was determined by induc-

Table 1. Magnesium concentration in the growth charge and LiNbO₃:Mg,B crystals and distribution coefficient K_d

Crystal	wt % Mg in the growth charge	wt % Mg in the crystal		K_d
		cone	tail end	
1	0.67	0.64	0.63	0.96
2	0.67	0.65	0.64	0.97

tively coupled plasma mass spectrometry (ICP MS) with an accuracy of $\sim 10^{-6}$ wt %. Mg concentration was evaluated by atomic emission spectroscopy (ICPS-9000, Shimadzu) with an accuracy of $\sim 10^{-3}$ wt %. The phase composition of the growth charge was determined by X-ray diffraction on a DRON-2 diffractometer (CuK radiation, graphite monochromator).

LiNbO₃:Mg,B crystals were grown in the [001] direction by the Czochralski technique from 85-mm-diameter platinum crucibles in air, using a Kristall-2 furnace. The heating unit design ensured an axial temperature gradient of $\sim 3^\circ\text{C}/\text{mm}$ over the melt in combination with an extended isothermal region in the post-growth annealing zone. The translation rate was 0.6 mm/h, and the rotation rate was 12 rpm, which ensured a flat solidification front. To relieve the thermoelastic stress, the crystals were heat-treated at 1230°C for 15 h. The heating/cooling rate was $\sim 50^\circ\text{C}/\text{h}$. To determine the dopant concentrations, plates ~ 0.8 mm in thickness were cut from the upper (cone) and lower (tail end) parts of each boule for the preparation of powder samples.

The rest of the LiNbO₃:Mg,B crystal was converted to a single-domain state via high-temperature electrodiffusion annealing during cooling of the samples at a rate of $\sim 20^\circ\text{C}/\text{h}$ in the temperature range from ~ 1235 to 735°C in a dc electric field. The degree of conversion into a single-domain state (degree of unipolarity) was evaluated from amplitude–frequency response curves and by static d_{333} piezoelectric modulus measurements. The optical quality of the crystals was assessed by counting the number of scattering centers in a laser beam using a procedure described previously [12].

In photoinduced light scattering (PILS) and laser conoscopy experiments, we used a Nd:YAG laser (MLL-100, Changchun New Industries Optoelectronics, China, $\lambda = 532$ nm, I up to ~ 6.29 W/cm²). More detailed descriptions of the PILS and laser conoscopy characterization techniques and the block diagrams of the experimental setups used in this study can be found in Palatnikov et al. [13].

RESULTS AND DISCUSSION

For LiNbO₃:Mg,B crystal growth, we prepared a granulated charge with a loose bulk density of

2.8 g/cm³. According to X-ray diffraction data, the growth charge corresponded to single-phase LiNbO₃. The phases present were identified using the ICDD database (PDF 4, release 2020, card no. 04-009-8480). The growth charge contained ~ 0.67 wt % Mg and 0.009 wt % B, which roughly corresponded to dopant concentrations in the homogeneously doped growth charge used in a previous study [10]. We grew two LiNbO₃:Mg,B crystals, 1 and 2, weighing 148.1 and 147.2 g, respectively, ~ 34 mm in diameter, with an ~ 20 -mm-long cylindrical body. The total weight of the growth charge in the crucible was 1775 g. No more than 8% of the melt was used for the growth of the crystals.

Mg concentration in the melt (C_m) for the growth of the next crystal and the effective dopant distribution coefficient (K_{eff}) were evaluated as described previously [13, 14]. The results are presented in Table 1. Analysis of the data in Table 1 indicates that direct solid-state synthesis of a growth charge from a Li₂CO₃ + Nb₂O₅ + MgO + H₃BO₃ mixture allows crystals with high chemical homogeneity to be grown: Mg concentration was shown to decrease by just ~ 0.01 wt % in going from the cone to the tail end. In the case of crystal growth from a melt containing ~ 0.67 wt % Mg (~ 3.9 mol % Mg), K_d was ~ 0.96 – 0.97 .

In a study of LiNbO₃:Mg crystals [6], it was shown that chemical homogeneity was only reached in the case of crystal growth from a melt containing ~ 4.6 – 5.3 mol % Mg, which was interpreted in terms of the structure and types of ionic complexes in the melt. If the melt contained < 4.6 mol % Mg, attempts to grow chemically homogeneous LiNbO₃:Mg crystals were unsuccessful [6]. Since the boron and magnesium dopants in the melt–crystal (LiNbO₃:Mg,B) system have an additive effect, the Mg concentration in the melt at which crystals with a uniform dopant distribution can be grown is substantially lower (Table 1). Note that, according to the ICP MS results, boron concentration in the LiNbO₃:Mg,B crystals was as low as $\sim 10^{-5}$ wt %.

After conversion to a single-domain state, the end faces and base (x -cut) of the crystals were thoroughly polished. Figure 1 shows photographs of the LiNbO₃:Mg,B crystals. High-speed evaluation of optical quality from the number of scattering centers in a laser beam showed that the density of scattering centers in crystal 1 was ~ 1.27 cm⁻³ (Table 2). In crystal 1, an imperfect region ~ 1 mm in thickness, with a rather high density of scattering centers, was detected ~ 1.5 cm from the cone. The imperfect region was located near a so-called “waist”—a local change in the diameter of the cylindrical body of the crystal—which probably originated from a short-term instability of growth conditions. At the same time, no scattering centers were detected in the bulk of crystal 2 (Table 2).

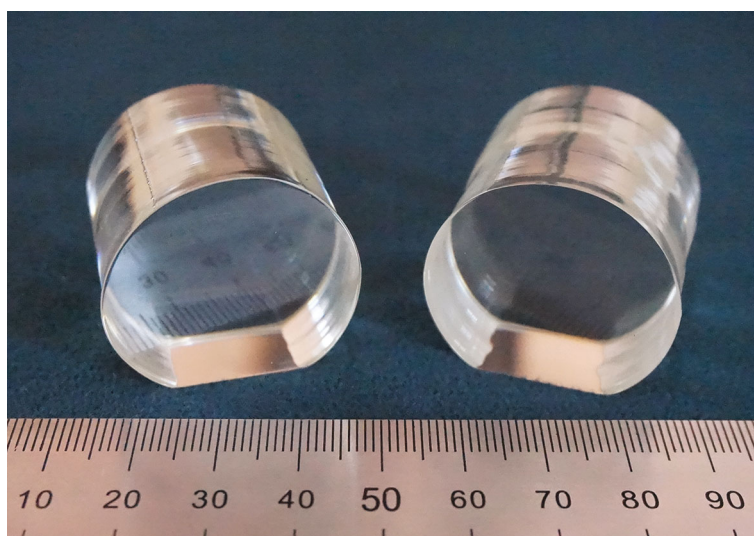


Fig. 1. Appearance of the $\text{LiNbO}_3:\text{Mg,B}$ crystals after conversion to a single-domain state and polishing.

Amplitude–frequency response (AFR) measurements showed that the main resonance peak in crystal *1* was located at a frequency of ~ 98.77 kHz and that the amplitude of the main resonance peak was eight times the background (Fig. 2a). In addition, the AFR curves had two secondary peaks at frequencies of ~ 117.93 and ~ 143.13 kHz, and one of them was a doublet. The AFR curve of crystal *2* had two resonance peaks (Fig. 2b). The main resonance was located at a frequency of ~ 95.25 kHz, and its amplitude exceeded the background by a factor of ~ 7.5 . A side electroacoustic resonance peak was located at a frequency of ~ 142.99 kHz. Both resonances of crystal *2* had a regular shape in the form of sharp peaks (Fig. 2b). The results of the AFR measurements for the $\text{LiNbO}_3:\text{Mg,B}$ crystals indicate that they were rather successfully converted to a single-domain state. The presence of two side resonances in the AFR curve of crystal *1* and the doublet shape of the latter resonance seem to be due to the “waist” in the cylindrical body of the crystal and the presence of residual microdomains in this region of the crystal. The piezoelectric modulus d_{333} , needed for assessing the degree of unipolarity of the crystals, was determined using an experimental setup for static piezoelectric effect measurements [15].

Figure 3 presents $Q_p(F)$ measurement results. The piezoelectric moduli d_{333} of crystal *1* (8.1 pC/N) and crystal *2* (8.6 pC/N) approach standard values ($d_{333} \geq 8$ pC/N according to Blistanov et al. [16]). The d_{333} of crystal *1* is somewhat smaller than that of crystal *2*. This seems to result from the presence of residual microdomains in the small “waist” region. Thus, the growth process was very sensitive to stability of its conditions, which was reflected in both the shape of the AFR curve and the d_{333} piezoelectric modulus (Figs. 2, 3). In the initial state, mechanical stress applied to a $\text{LiNbO}_3:\text{Mg,B}$ crystal induces a small polarization charge due to a weak native unipolarity of a polydomain crystal (Fig. 3, curve 3).

The PILS results for the $\text{LiNbO}_3:\text{Mg,B}$ crystals showed that they had rather high optical quality (Fig. 4). It is clearly seen in Fig. 4 that, even at a comparatively high excitation intensity (~ 6.29 W/cm²), there was no photorefractive response, the PILS indicatrix did not open, and no laser beam destruction occurred. This points to suppression of the photorefractive effect in the $\text{LiNbO}_3:\text{Mg,B}$ crystals *1* and *2*.

Macroscopic optical homogeneity of the $\text{LiNbO}_3:\text{Mg,B}$ crystals was assessed by laser conoscopy (Fig. 5). In spite of some distortion, mainly due to the

Table 2. High-speed optical quality assessment results for the $\text{LiNbO}_3:\text{Mg,B}$ crystals

Crystal	Total number of scattering centers	Average number of scattering centers per row	Density of scattering centers, cm ⁻³
<i>1</i>	0.67	0.64	0.63
<i>2</i>	0.67	0.65	0.64

The number of rows is 25.

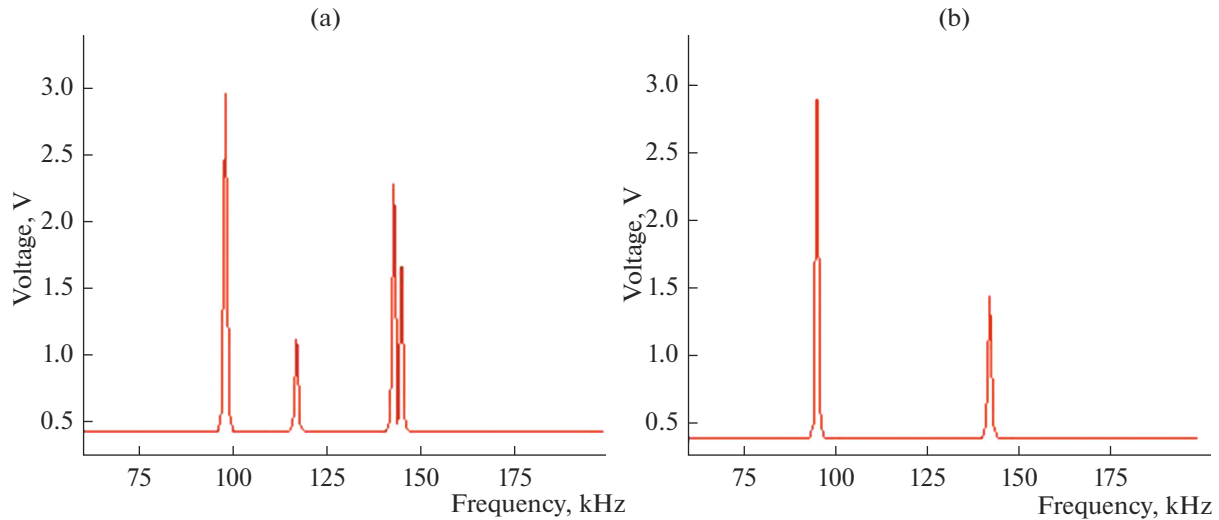


Fig. 2. AFR curves of the low-frequency part of the electromechanical spectrum of crystals (a) 1 and (b) 2.

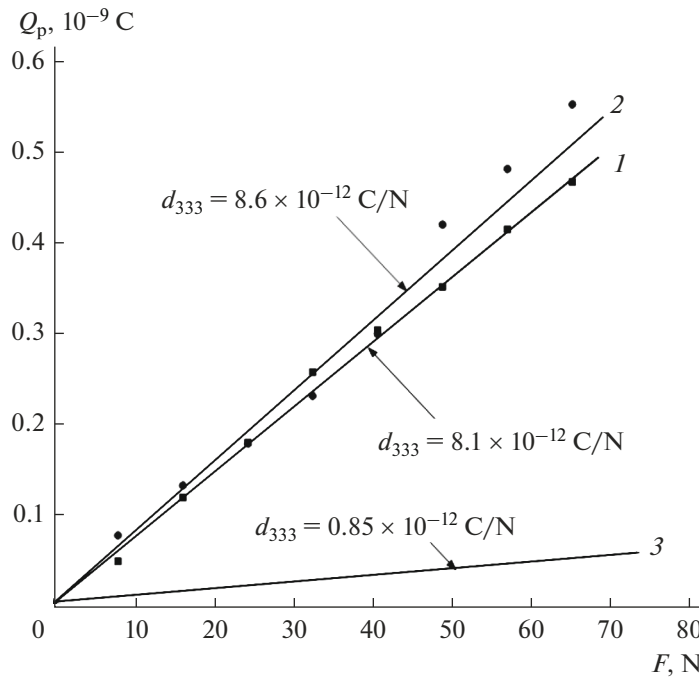


Fig. 3. Q_p as a function of F for crystals 1 and 2 after conversion to a single-domain state; (3) originally polydomain crystal 2.

large thickness of crystals 1 (~38 mm) and 2 (~40 mm) and the associated optical distortion accumulation during laser beam propagation, the conoscopic patterns of the LiNbO₃:Mg,B crystals showed that they had rather high optical quality. It is worth noting that, to examine conoscopic patterns, use is commonly made of plates 1 to 3 mm in thickness. In the present conoscopic patterns, the “Maltese cross” is slightly elongated in the horizontal (crystal 1) or vertical (crystal 2) direction, corresponding to the optical indicatrix distortion direction, with no discontinuity in the center of the cross. Moreover, isochromes retain the shape of concentric circles, without acquiring ellipticity (Fig. 5). The anomalies correspond to a small optical biaxiality due to the optical distortion accumulation during laser beam propagation. Raising the laser output power to 90 mW caused no further distortion of the conoscopic patterns. This suggests that the LiNbO₃:

tal 2) direction, corresponding to the optical indicatrix distortion direction, with no discontinuity in the center of the cross. Moreover, isochromes retain the shape of concentric circles, without acquiring ellipticity (Fig. 5). The anomalies correspond to a small optical biaxiality due to the optical distortion accumulation during laser beam propagation. Raising the laser output power to 90 mW caused no further distortion of the conoscopic patterns. This suggests that the LiNbO₃:

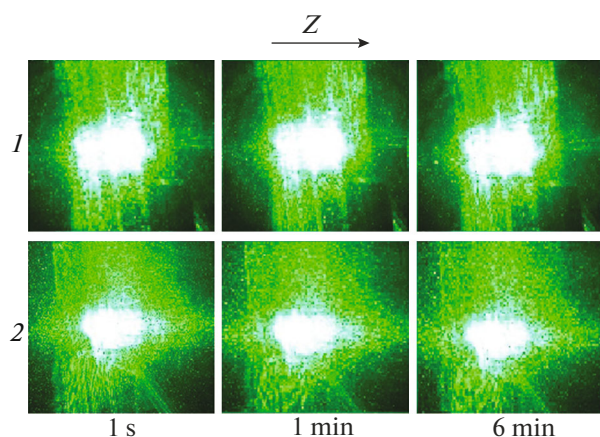


Fig. 4. PILS patterns of the $\text{LiNbO}_3\text{:Mg,B}$ crystals ($\lambda = 532$ nm, $I = 6.29$ W/cm²).

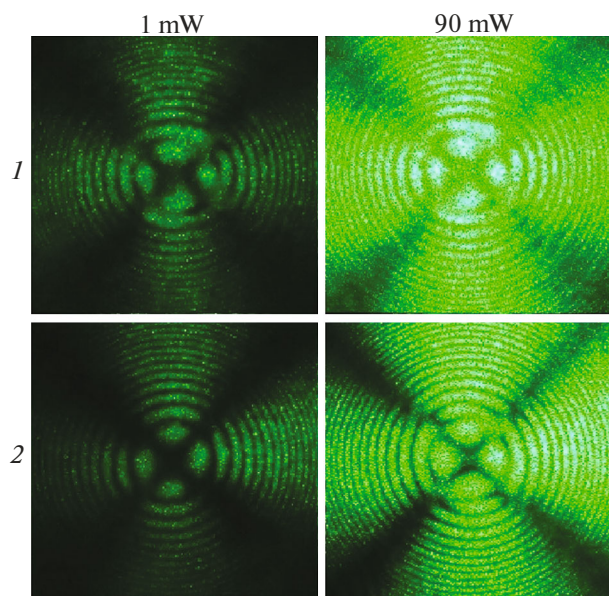


Fig. 5. Conoscopic patterns of crystals 1 and 2 ($\lambda = 532$ nm, $P = 1$ and 90 mW).

Mg,B crystals had no photorefractive response, as supported by the present PILS results (Fig. 4). The conoscopic patterns of crystal 1 are more imperfect than those of crystal 2, suggesting that crystal 2 has better optical homogeneity. This is due to the presence of an imperfect region in crystal 1 around the “waist”—a local change in the diameter of the cylindrical body of the crystal, which originated from a short-term instability of growth conditions.

CONCLUSIONS

A technologically feasible process has been designed for the preparation of a $\text{LiNbO}_3\text{:Mg,B}$ growth charge with preset dopant concentrations by

solid-state synthesis. We have found conditions for the growth of optical-quality $\text{LiNbO}_3\text{:Mg,B}$ crystals with a highly uniform dopant distribution.

Using AFR and d_{333} piezoelectric modulus measurements, we have demonstrated a high degree of unipolarity of the $\text{LiNbO}_3\text{:Mg,B}$ crystals. The present PILS results for the $\text{LiNbO}_3\text{:Mg,B}$ crystals confirm that they have high optical damage resistance, and the laser conoscopy results demonstrate that they have rather high optical homogeneity.

Thus, $\text{LiNbO}_3\text{:Mg,B}$ crystals can be regarded as a new optical material for laser light conversion.

CONFLICT OF INTEREST

The authors declare that they have no conflicts of interest.

REFERENCES

1. Kuz'minov, Yu.S., *Elektroopticheskii i nelineino-opticheskii kristall niobata litiya* (Electro-Optic and Nonlinear Optical Lithium Niobate Crystals), Moscow: Nauka, 1978.
2. Volk, T.R. and Wohlecke, M., Optical damage resistance in LiNbO_3 crystals, *J. Ferroelectrics Rev.*, 1998, vol. 1, pp. 195–262.
3. Zhang, Q.-R. and Feng, X.-Q., Defect structures and the MgO-doped-level-threshold affect on the optical absorption of reduced MgO-doped lithium niobate, *Phys. Rev. B: Condens. Matter Mater. Phys.*, 1991, vol. 43, no. 14, pp. 12019–12024.
4. Kim, I.W., Park, B.C., Jin, B.M., Bhalla, A.S., and Kim, J.W., Characteristics of MgO-doped LiNbO_3 crystals, *Mater. Lett.*, 1995, vol. 24, pp. 157–160.
5. Choubey, R.K., Sen, P.K., Bhatt, R., and Kar, S., Optical properties of MgO-doped LiNbO_3 single crystals, *Opt. Mater.*, 2006, vol. 28, pp. 467–472.
6. Palatnikov, M.N., Biryukova, I.V., Makarova, O.V., Sidorov, N.V., Kravchenko, O.E., and Efremov, V.V., Growth of large $\text{LiNbO}_3\text{:Mg}$ crystals, *Inorg. Mater.*, 2013, vol. 49, no. 3, pp. 288–295.
7. Palatnikov, M.N., Sidorov, N.V., Titov, R.A., Teplyakova, N.A., and Makarova, O.V., Physicochemical and optical characteristics of boron-doped LiNbO_3 single crystals, *Perspekt. Mater.*, 2018, no. 6, pp. 5–15.
8. Makarova, O.V., Palatnikov, M.N., Biryukova, I.V., Teplyakova, N.A., and Sidorov, N.V., Structure and properties of boron-doped LiNbO_3 single crystals, *Inorg. Mater.*, 2018, vol. 54, no. 1, pp. 49–54.
9. Sidorov, N.V., Teplyakova, N.A., Makarova, O.V., Palatnikov, M.N., Titov, R.A., Manukovskaya, D.V., and Biryukova, I.V., Boron influence on defect structure and properties of lithium niobate crystals, *Crystals*, 2021, vol. 11, pp. 458–490.
10. Masloboeva, S.M., Efremov, I.N., Biryukova, I.V., and Palatnikov, M.N., Preparation and characterization of lithium niobate single crystals activated with magnesium and boron, *Inorg. Mater.*, 2021, vol. 57, no. 12, pp. 1271–1278.

11. Palatnikov, M.N., Sidorov, N.V., and Kalinnikov, V.T., *Segnetoelektricheskie tverdye rastvory na osnove oksidnykh soedinenii niobiya i tantala: sintez, issledovanie strukturnogo uporyadocheniya i fizicheskikh kharakteristik* (Ferroelectric Solid Solutions Based on Niobium and Tantalum Oxide Compounds: Synthesis, Structural Ordering, and Physical Characterization), St. Petersburg: Nauka, 2002, 2nd ed.
12. Masloboeva, S.M., Efremov, I.N., Biryukova, I.V., and Palatnikov, M.N., Growth and characterization of a boron-doped lithium niobate single crystal, *Inorg. Mater.*, 2020, vol. 56, no. 11, pp. 1147–1152.
13. Palatnikov, M.N., Sidorov, N.V., Kadetova, A.V., Teplyakova, N.A., Makarova, O.V., and Manukovskaya, D.V., Concentration threshold in optically nonlinear LiNbO₃:Tb crystals, *Opt. Laser Technol.*, 2021, vol. 137, paper 106821.
14. Palatnikov, M.N., Biryukova, I.V., Makarova, O.V., Efremov, V.V., Kravchenko, O.E., Skiba, V.I., Sidorov, N.V., and Efremov, I.N., Growth of heavily doped LiNbO₃:Zn crystals, *Inorg. Mater.*, 2015, vol. 51, no. 4, pp. 375–379.
15. Palatnikov, M.N., Sandler, V.A., Sidorov, N.V., Efremov, I.N., and Makarova, O.V., Methods for controlling the degree of unipolarity of large LiNbO₃ crystals, *Instrum. Exp. Tech.*, 2020, no. 3, pp. 383–387.
16. Blistanov, A.A., Bondarenko, V.S., Perelomova, N.V., Strizhevskaya, F.N., Chkalova, V.V., and Shaskol'skaya, M.P., *Akusticheskie kristally. Spravochnik* (Acoustic Crystals: A Handbook), Shaskol'skaya, M.P., Ed., Moscow: Nauka, 1982.

Translated by O. Tsarev